

DTIC FILE COPY

4

# David Taylor Research Center

Bethesda, MD 20084-5000

DTRC/SHD-1268-03

AD-A202 674

DTRC/SHD-1268-03

DEC -- 1988

SHIP HYDROMECHANICS DEPARTMENT

DEPARTMENTAL REPORT

ANALYSIS OF PROPELLER WAKE FLOW VISUALIZATION  
NEAR A FREE SURFACE

By

Scott Fish  
James N. Blanton

ANALYSIS OF PROPELLER WAKE FLOW VISUALIZATION  
NEAR A FREE SURFACE



APPROVED FOR PUBLIC RELEASE  
DISTRIBUTION UNLIMITED

DTIC  
ELECTE  
S 19 JAN 1989 D  
E

89 1 18 092

## MAJOR DTRC TECHNICAL COMPONENTS

- CODE 011 DIRECTOR OF TECHNOLOGY, PLANS AND ASSESSMENT
- 12 SHIP SYSTEMS INTEGRATION DEPARTMENT
- 14 SHIP ELECTROMAGNETIC SIGNATURES DEPARTMENT
- 15 SHIP HYDROMECHANICS DEPARTMENT
- 16 AVIATION DEPARTMENT
- 17 SHIP STRUCTURES AND PROTECTION DEPARTMENT
- 18 COMPUTATION, MATHEMATICS & LOGISTICS DEPARTMENT
- 19 SHIP ACOUSTICS DEPARTMENT
- 27 PROPULSION AND AUXILIARY SYSTEMS DEPARTMENT
- 28 SHIP MATERIALS ENGINEERING DEPARTMENT

This document contains information affecting the national defense of the United States within the meaning of the **Espionage Laws, Title 18, U.S.C.**, Sections 793 and 794. The transmission or revelation of its contents in any manner to an unauthorized person is prohibited by law.

### DTRC ISSUES THREE TYPES OF REPORTS:

1. **DTRC reports, a formal series**, contain information of permanent technical value. They carry a consecutive numerical identification regardless of their classification or the originating department.
2. **Departmental reports, a semiformal series**, contain information of a preliminary, temporary, or proprietary nature or of limited interest or significance. They carry a departmental alphanumerical identification.
3. **Technical memoranda, an informal series**, contain technical documentation of limited use and interest. They are primarily working papers intended for internal use. They carry an identifying number which indicates their type and the numerical code of the originating department. Any distribution outside DTRC must be approved by the head of the originating department on a case-by-case basis.

UNCLASSIFIED

SECURITY CLASSIFICATION OF THIS PAGE

REPORT DOCUMENTATION PAGE

1a. REPORT SECURITY CLASSIFICATION UNCLASSIFIED		1b. RESTRICTIVE MARKINGS	
2a. SECURITY CLASSIFICATION AUTHORITY		3. DISTRIBUTION/AVAILABILITY OF REPORT	
2b. DECLASSIFICATION/DOWNGRADING SCHEDULE		STATEMENT A	
4. PERFORMING ORGANIZATION REPORT NUMBER(S) DTRC/SHD-1268-03		5. MONITORING ORGANIZATION REPORT NUMBER(S)	
6a. NAME OF PERFORMING ORGANIZATION David Taylor Research Center	6b. OFFICE SYMBOL (If applicable) Code 1543	7a. NAME OF MONITORING ORGANIZATION	
6c. ADDRESS (City, State, and ZIP Code) Bethesda, MD, 20084-5000		7b. ADDRESS (City, State, and ZIP Code)	
8a. NAME OF FUNDING/SPONSORING ORGANIZATION Office of Naval Research	8b. OFFICE SYMBOL (If applicable)	9. PROCUREMENT INSTRUMENT IDENTIFICATION NUMBER	
8c. ADDRESS (City, State, and ZIP Code) Alexandria, VA 22217		10. SOURCE OF FUNDING NUMBERS	
		PROGRAM ELEMENT NO. 61153N	PROJECT NO.
		TASK NO. BT02301N1	WORK UNIT ACCESSION NO. DN50716
11. TITLE (Include Security Classification) Analysis of Propeller Wake Flow Visualization Near a Free Surface			
12. PERSONAL AUTHOR(S) Scott Fish, James N. Blanton			
13a. TYPE OF REPORT Technical	13b. TIME COVERED FROM 1/88 TO 9/88	14. DATE OF REPORT (Year, Month, Day) 1988 November	15. PAGE COUNT 31
16. SUPPLEMENTARY NOTATION			
17. COSATI CODES		18. SUBJECT TERMS (Continue on reverse if necessary and identify by block number)	
FIELD	GROUP	SUB-GROUP	
		Propeller Wake	
		Vortex Kinematics; → Flow Visualization. (cdc) ←	
19. ABSTRACT (Continue on reverse if necessary and identify by block number) → Propeller wake flow visualization was carried out for several depths of submergence below a free surface. The wake was visualized by laser light sheet illumination of the blade tip vortex helix seeded with fluorescein dye. Effects of the free surface on the propeller wake were seen at the shallower submergence depths. Instability in the helix was apparent at much shorter distances downstream than has previously been observed in cavitation experiments. The dominant cause of this instability is determined to be caused by the use of inclined universal joints in the propeller drive system. A simple test modification is described for the elimination of this influence. Estimation of Reynolds number, submergence depth, and propeller loading influences on the propeller wake are given. Keywords: Marine Propellers wake; /			
20. DISTRIBUTION/AVAILABILITY OF ABSTRACT <input type="checkbox"/> UNCLASSIFIED/DUNLIMITED <input checked="" type="checkbox"/> SAME AS RPT <input type="checkbox"/> DTIC USERS		21. ABSTRACT SECURITY CLASSIFICATION UNCLASSIFIED	
22a. NAME OF RESPONSIBLE INDIVIDUAL		22b. TELEPHONE (Include Area Code)	22c. OFFICE SYMBOL

## CONTENTS

NOTATION .....	v
ABSTRACT .....	1
ADMINISTRATIVE INFORMATION .....	1
INTRODUCTION .....	1
EXPERIMENTAL ARRANGEMENT .....	2
DYE INJECTION FLOW VISUALIZATION .....	4
WAKE HELIX INSTABILITY .....	5
PRESENTATION OF RESULTS .....	9
REYNOLDS NUMBER DEPENDENCE .....	9
PROPELLER LOADING VARIATION .....	10
PROPELLER DEPTH VARIATION .....	13
<u>Propeller Wake Influence</u> .....	13
<u>Free Surface Influence</u> .....	14
WAKE PERSISTENCE .....	16
DISCUSSION AND RECOMMENDATIONS .....	17
REFERENCES .....	31

<b>Accession For</b>	
NTIS GRA&I	<input checked="" type="checkbox"/>
DTIC TAB	<input type="checkbox"/>
Unannounced	<input type="checkbox"/>
Justification	
By _____	
Distribution/	
Availability Codes	
Dist	Avail and/or Special
<b>A-1</b>	



## FIGURES

Fig. 1. Four bladed propeller with hollow hub and dye slotted blades . . . . .	19
Fig. 2. Experimental configuration . . . . .	20
Fig. 3. Laser light sheet and video camera configuration . . . . .	21
Fig. 4. Video frames of vortex twisting, $J=0.5$ , 0.1 second increments . . . . .	22
Fig. 5. Angular position of motor drive shaft and propeller . . . . .	23
Fig. 6. Three-dimensional view of tip vortex helix . . . . .	24
Fig. 7. Wake video frames for different $Re_{a,7}$ . . . . .	25
Fig. 8. Wake video frames: $J$ variation, $z_{hub}/R=2.0$ . . . . .	27
Fig. 9. Calculated blade loading and vortex spacing versus $J$ . . . . .	26
Fig. 10. Induced velocity variation . . . . .	26
Fig. 11. Comparison of calculated and measured streamwise wake length scale . . . . .	28
Fig. 12. Wake video frames: shallow submergence, $z_{hub}/R=1.25$ , $J=0.5$ . . . . .	29

## TABLES

Table 1. Free surface effects due to struts and pod: $z_{hub}/R=1.25$ . . . . .	30
---	----

## NOTATION

A	Amplitude of angular variation oscillation
D	Propeller diameter
$C_{\tau}$	Propeller blade chord length at $r/R=0.7$
J	Advance ratio = $U_{\text{car}}/nD$
$l_1$	Downstream propeller wake surface contact length
L	Lift force on blade / span of blade
n	Propeller rps
r	Radial coordinate
R	Propeller radius
Re	Reynolds number = $UD/\nu$
$Re_{\tau}$	Reynolds number based on 0.7R blade chord = $C_{\tau} [U_{\text{car}}^2 + (0.7nD\pi)^2]^{0.5} / \nu$
$U_{\text{car}}$	Carriage velocity
x	Streamwise distance from plane of propeller blade midchords
$z_{\text{hub}}$	Depth of hub axis from free surface
$\beta$	Wake spreading angle
$\Gamma$	Vortex strength = $L/\rho U$
$\nu$	Kinematic viscosity
$\theta_p$	Angular displacement of propeller
$\theta_m$	Angular displacement of motor drive shaft
$\rho$	Density
$\omega_p$	Angular velocity of propeller
$\omega_m$	Angular velocity of motor drive shaft

## ABSTRACT

Propeller wake flow visualization was carried out for several depths of submergence below a free surface. The wake was visualized by laser light sheet illumination of the blade tip vortex helix seeded with fluorescein dye. Effects of the free surface on the propeller wake were seen at the shallower submergence depths. Instability in the helix was apparent at much shorter distances downstream than has previously been observed in cavitation experiments. The dominant cause of this instability is determined to be caused by the use of inclined universal joints in the propeller drive system. A simple test modification is described for the elimination of this influence. Estimation of Reynolds number, submergence depth, and propeller loading influences on the propeller wake are given.

## ADMINISTRATIVE INFORMATION

The work described in this report is part of the Surface Ship Wake Consortium sponsored by the Office of Naval Research (ONR), under Program Element 61153N, Task Area BT02301N1, and performed under the David Taylor Research Center (DTRC) work unit 1-1504-200 (FY 88). Additional funds were provided by the 6.2 Ship and Submarine Technology Program, Program element 62543N, Task area SF 43421 for analysis of the experimental results and publication of this report.

## INTRODUCTION

Recent studies suggest that the interaction of turbulence in a ship's wake with the free surface may define characteristics of some parts of the ship hydrodynamic signature (Lyden, et al., 1985). As a major producer of turbulence in the ship's wake, the propeller deserves careful examination to determine both the character of its turbulent wake and the resulting influence this wake has on the free surface. Velocity measurements made at David Taylor Research Center (DTRC) have shown a lack of blade rate periodicity in the

propeller wake beyond five propeller diameters downstream (Blanton and Fish, 1988). This degradation of blade rate dependence suggests either turbulent diffusion of the individual blade wakes or an instability in flow geometry disturbing the wake axisymmetry. Photographs of propellers cavitating in water tunnels have shown very symmetric helical structure in the propeller wake. Water tunnel photographs are typically limited in downstream viewing range to  $x/D=2.0$  (Kuiper, 1979). In addition, the tunnel walls may provide some stabilizing effect on the propeller wake geometry. In order to examine the interaction of the propeller wake with a free surface, the structure of the wake should be identified and understood. This understanding is of fundamental importance in validating numerical prediction codes aimed at simulating the propeller wake interaction with the free surface. Due to the complicated nature of this flow field, a visual perspective on the wake evolution was deemed necessary prior to any detailed wake survey measurements.

This report reviews flow visualization data collected on a propeller wake operating at two depths below a free surface. High contrast black and white video coverage showing laser light sheet illumination of the tip vortex helical wake were recorded for a variety of operating conditions. Screen images are included here with associated comments. A preliminary report, Fish and Blanton (1988), provided initial presentation and analysis of this experiment.

## EXPERIMENTAL ARRANGEMENT

The David Taylor Research Center 140 foot Towing Basin was used for the experiments presented in this report. Although the carriage was operated at speeds from 1 to 4 ft/sec (0.305 to 1.22 m/sec), the data presented here, except where noted, were taken at a carriage speed of 1 ft/sec (0.305 m/sec) for maximum dye clarity.

A four bladed, 12 in. diameter propeller (DTRC #3563) was used. This propeller was modified by milling a 1/8 in. (0.3175 cm) wide slot in each blade face. The milled slot was then covered with tape to form a passage for dye from the hub to the blade tip as shown in Fig. 1. The 0.002 in (0.1 mm) thickness of the tape was assumed small enough to maintain the original blade face geometry and resulting propeller performance.

A tri-strut and pod configuration was designed and built to minimize both the free surface disturbance and the propeller inflow asymmetry while maintaining structural rigidity (see Fig. 2). The propeller drive motor was remotely located on the carriage and connected to the hollow prop shaft through a 3/8 in. (0.95 cm) angle drive shaft positioned just forward of the center strut. U-joints on either end of the angle drive shaft were aligned to minimize angular velocity variations (no visual differences in angular velocity were initially apparent; see WAKE HELIX INSTABILITY section).

A variable speed positive displacement pump supplied a fluorescein dye solution to the pod. The fluorescein dye was illuminated using a laser light sheet, positioned as shown in Fig. 3. The light sheet was created using a 110 mW argon-ion laser directed into a 30 Hz vibrating mirror. This sheet was fixed (not moving with the carriage) in the vertical plane and aligned with the propeller axis.

A Sony 3/4 in., 30 frame per second video tape recorder was used to record images from a high sensitivity black and white camera mounted on the basin side as shown in Fig. 3. The images shown here are 35 mm photographs of the video screen.

## DYE INJECTION FLOW VISUALIZATION

The dye injection rate was examined to determine its influence on the formation of the tip vortex. Care was taken to balance the need for maximum dye flow rate producing extended wake visualization time with the need for minimum dye flow rate disturbance of the flow in the blade tip region. Selection of an "optimum" dye delivery flow rate was made after recording wake images under a variety of dye flow rates and propeller rotation speeds. "Optimum" here was defined as the minimum flow rate giving sufficient dye in the vortices for sharp contrast to one diameter downstream. Dye pump speed variation about this small flow rate had no apparent influence on the vortex wake. The resulting flow rate of 0.394 in<sup>3</sup>/sec (6.45 ml/sec) gave an estimated radial velocity on the blade face exit point of 16.8 in./sec (43 cm/sec). This exit velocity is approximately one third of the circumferential velocity at the tip and is oriented in the same direction as the radial flow induced by the tip vortex. Recall that the dye slot is on the face or "pressure" side of the blade.

Dye injection rates were increased only in select high speed/low  $J$  cases in order to enhance the video contrast. In these cases, no apparent changes were noticed in the flow, only sharper contrast in the images. The large variation in exit velocity of the dye caused by the flow rate change indicated that under these circumstances, the momentum transfer from the dye exit point had a negligible effect on the formation of the tip vortex.

Care must be taken in interpreting dye roll-up as discrete vortices. As shown by Hama (1962) and recently by Cimbala et al. (1988), streakline dye patterns show the integrated motion of the marked fluid from its point of introduction. In the current experiment, however, local rates of change of the dye roll-up were sufficient to indicate

persistent vortical structure. The continuous change in the dye roll-up provided an accurate marker of the fluid velocity. Comparison with the velocity field induced by discrete vortex lines leads to accurate location estimates of the vorticity centers.

#### WAKE HELIX INSTABILITY

The most striking feature illustrated in the video coverage in this experiment was the twisting of vortex structures in pairs resembling a 2-dimensional vortex "pairing" phenomenon (Ho and Huerre, 1984) in the plane of the laser light sheet. This flow phenomenon will be referred to as *vortex twisting* and will be described further in the following paragraphs. Fig. 4 shows a time sequence of the helix in 0.1 second increments. The propeller loading corresponds to  $J=0.5$ . The dye spots marking the vortex cores can be seen to pair up and rotate about each other as the propeller moves further to the right of the photographs. If the wake were to remain stable and symmetric, the dye spots would remain roughly equidistant from each other, appearing similar to a discretised vortex sheet. The movement of these dye spots therefore indicates a loss of symmetry caused by an unsteady influence on the propeller wake. This type of vortex motion appeared in all of the operating conditions of this experiment except at the non-loaded advance ratio. Details of any differences are described in later sections of this report. Although previous analytic work indicated the inherent instability of helical vortices (Widnall 1972), propeller tip vortex cavitation observations in water tunnels have shown stable helix forms. To determine the nature of the observed vortex twisting, an evaluation of possible influences on propeller wake instability was conducted.

Sources of unsteady perturbation on propeller wake flow fields are listed below:

- a. unsteady propeller inflow
- b. non-uniform spatial propeller inflow
- c. flow asymmetry caused by the free surface
- d. unsteady rotation of propeller
- e. blade-to-blade variations in loading

It should be noted that item d can be modeled as a combination of items a and b.

Item e, blade-to-blade loading variations, could be caused by geometric variations between the blades, or by variations in the boundary layer flow pattern over similarly shaped blades. Dimensional measurements of the propeller however, showed very uniform blade geometries. In addition, no roughness variations were found from blade-to-blade which might cause boundary layer transition/separation variations.

Since these experiments were conducted in a still water towing tank, the turbulence level was observed to be extremely low and spatially uniform prior to each run. The influence of the strut wakes on the wake helix could not be neglected, but appeared to be insignificant judging by the similarity of vortex twisting in the lower region near the propeller (no strut effect) to that of the upper region near the propeller (See Fig. 4). The effect of strut wakes, if any, would be seen in this region. Any inflow unsteadiness was therefore suspected to be due to carriage motions or propeller drive unsteadiness. Although vibrations on the carriage were not measured, the same form of unsteady flow was observed over wide variations in both carriage speed and blade rate frequencies. The similarity of the flow unsteadiness under these conditions implied a negligibly low influence of unsteady carriage motions.

To determine if an unsteady perturbation of the flow field was being created by the propeller drive system, careful measurements of the angular motion of the propeller were made. Fig. 5 shows results of a comparative measurement of the angular positions of the motor drive shaft  $\theta$ , and the propeller  $\theta_p$ . The two-cycle nature of the curve is a characteristic of the non-constant angular transmission of the two inclined universal joints. Despite their ease in design application, universal joints in this inclined fashion were found to cause an undesirable unsteady angular velocity.

An analysis shows how this small unsteady angular velocity variation can dominate the downstream interaction of the propeller tip vortices and could give rise to the vortex twisting observed in this experiment. The key to the analysis is the coincidence of the four lobes (upper and lower peaks) in the angular velocity,  $\omega$ , with the positions of the four blades of the propeller. A typical sequence of blade passages through a fixed angular position can help in visualizing the significance of this result.

- a. Assume that blade #1 passes through the vertical position when the propeller is operating at the positive peak of  $\omega$  variation.
- b. Blade #2 will pass through the vertical position 90 degrees later, but now the propeller is operating at the negative peak of angular velocity.
- c. Blade #3 passes vertical 180 degrees later and the propeller is again at the positive peak of  $\omega$  similar to when blade #1 passed through the vertical position.
- d. Finally blade #4 passes through vertical with the minimum  $\omega$  similar to when blade # 2 passed through vertical.

In other words, the 180 degree separation of every other blade synchronizes with the 180 degree separation in positive (or negative) peaks in the angular velocity curve. The net result is an oscillation (at each fixed angular position) of the instantaneous value of propeller advance ratio. In this experiment, the light sheet focuses the viewer's attention on two discrete positions: top and bottom. The visible vortices shed into the wake will therefore alternate in strength and position based on the advance ratio,  $J$ , of the propeller at the instant the blade passes through the sheet. With these conditions defined, one can derive a vortex interaction scenario for comparison with the observations.

The fluctuations in  $J$  caused by the  $\omega$  oscillation give rise to changes in the axial compression of the vortex helix geometry. A tip vortex will experience an imbalance in induced velocity from its neighboring blade tip vortices due to their unequal spacing. If the closest neighbor vortex is downstream, the net induced motion will be radially inward. The significance of this inward motion arises from the high radial gradient in axial velocity in the tip vortex region. This gradient causes filaments of lower radial position to be convected downstream faster than their partners at higher radial position. This convection can be visualized in both the 3-Dimensional images of Fig. 6 and the laser light sheet images (see Fig. 4). Note in Fig. 4 the relative movement of the dye spots labeled "1" and "2". Despite their similar motion to vortex "pairing", it should be remembered that the twisting process as shown in Fig. 6 is very 3-dimensional.

The continued interaction of the vortices once they have been shed was seen to be dependant on the propeller loading and is discussed further in the PROPELLER LOADING VARIATION section.

The dominance of unsteady angular velocity in the propeller wake will be eliminated in future experiments through the use of constant velocity joints. Despite the inclusion of this unsteady  $\omega$  variation, the results obtained from the present study will be useful in the study of propeller wakes near a free surface.

## PRESENTATION OF RESULTS

### REYNOLDS NUMBER DEPENDENCE

Experimental measurements such as (Cook, 1972) have shown that tip vortices can be modelled with finite radius viscous cores, outside of which the flow behaves in an inviscid manner. The existence of a viscous core leads one to examine the Reynolds number dependence of results utilizing visualization of these vortices. A series of cases was therefore recorded for several carriage speeds while varying the rpm to maintain the same advance coefficient,  $J$ . The resulting increase in flow speed over the blades could therefore be examined without changing the flow angle of attack. This allowed observation of wake variations due to viscous effects. This comparison was made only with the deep model submergence (minimizing Froude number effects due to free surface waves).

Fig. 7 isolates the upper row of wake vortices at  $J=0.8$  for three different  $Re_{a,7}$  ranging from  $\approx 1.3 \times 10^5$  to  $\approx 2.6 \times 10^5$ . Although the rate of dye diffusion is greater for the higher  $Re_{a,7}$ , the trajectory and pairing of the vortices are essentially the same. This indicates that under the conditions of this test, the Reynolds number effects were overshadowed by the effect of the angular velocity variation described previously in the WAKE HELIX INSTABILITY section.

Reynolds numbers ( $Re_{a,7}$ ) for the propeller varied from  $\approx 5 \times 10^4$  to  $\approx 1.5 \times 10^5$  for a carriage velocity of 1 ft/s. Meyne (1972) reports, for similar 4-bladed propellers, the

pressure side remained laminar up to  $Re_{a,7} = 8 \times 10^5$ , and the suction side remained laminar between  $Re_{a,7} = 2 \times 10^5$  and  $Re_{a,7} = 3 \times 10^5$ , depending on advance coefficient. This suggests that the visualization data for the 1 ft/sec carriage speed corresponds to laminar flow over the entire propeller.

As the Reynolds number is increased, the laminar tip vortices will transition to turbulent flow at smaller axial distances downstream (see Fig. 7). In order to reveal any effects of laminar to turbulent vortex transition on the wake interaction process, however, the propeller drive modifications to remove unsteady  $\omega$  variations will be needed. The constant propeller angular velocity should give rise to a more symmetric vortex wake, increasing the importance of viscous and gravitational forces in the wake vorticity kinematics.

#### PROPELLER LOADING VARIATION

The principal parameter varied through this experiment besides the propeller submergence depth was the propeller loading condition. This was done by holding the carriage speed constant and changing the rotational speed of the drive shaft. This changed the advance ratio,  $J$ , representing the angle of attack and resultant loading on the propeller blades. By systematically observing the wake under various loading conditions, wake behavior for variations in propeller jet strength could be evaluated.

The comparison in Fig. 8 ( $J$  ranging from 0.8 to 0.4) shows the strong dependence on  $J$  of the vortex twisting process. The most obvious effect of lowering  $J$  is the decrease in streamwise length scale (or time scale) of the twisting motion. The apparent symmetry between the top and bottom rows of vortices indicates negligible influence of the free surface or the support struts at this deep submergence depth ( $z_{sub}/R=2$ ). The influence of

propeller loading on the vortex interaction process was therefore pursued through closer examination of wake images under various  $J$  conditions.

Since  $J$  was usually varied by changing propeller shaft angular velocity under a constant carriage speed, the influence of unsteady rotation caused by the universal joints would also need consideration. The influence of angular velocity on  $J$  can be determined from the definition:  $J = U / (nD) = 2\pi U / (\omega_p D)$ . Computation of the helical vortex spacing for each  $J$  can be made using simple geometry. Estimates of the propeller blade load can also be made using the open water propeller loading curves. The trends in calculated vortex spacing and blade loading for variations in  $J$  are shown in Fig. 9. An estimate of the tip vortex strength can be made using the blade loading by assuming that all of the bound vorticity in the blade is shed and rolled up into the tip vortex. The tip vortex strength is known then from:  $\Gamma = L/(\rho U)$  (where:  $L$  = lift force on blade / span of blade). Note that the lift force on the blade can be estimated from the open water curves for a known  $J$  value. Combining the estimated vortex strength and separations with the Biot-Savart law gives estimates of the induced velocity of the vortices. Computed trends in the wake vortex-induced velocity with respect to  $J$  are plotted in Fig. 10. Induced velocities calculated here utilize simplified assumptions of low vortex curvature (essentially 2-dimensional) but illustrate the trend of a full 3-dimensional analysis. Note especially the increasing trend in induced velocity between the vortices as  $J$  is reduced. The higher induced velocities at low  $J$  values speed up the twisting process once perturbations are applied. The effect is similar to the growth in numerical instability of filament models of vortex sheet motions as the filament spacing is reduced or strength increased as described in Moore (1971).

Using this induced velocity trend, a streamwise length scale can be calculated and compared with length scale measurements from the video images. The measurement used for comparison is the streamwise distance from the propeller plane to the plane where a vortex pair has first reached a vertical orientation. Fig. 11 shows a comparison of calculated length scale (normalized to match the measured data at  $J=0.5$ ) with the measured length scale. The agreement is reasonably good considering the calculations are derived from a 2-dimensional model of the vortex interaction, and neglects the increase in induced velocity caused by the unsteady shaft rotation at lower  $J$  (see Fig. 10) and decrease in induced velocity caused by self-induced velocities of curved vortex filaments. The calculations at the very least confirm that the twisting length should be reduced as  $J$  is reduced.

An additional difference in the vortex interaction was noted at the lower  $J$  values. At  $J=0.4$  the larger radial gradient in streamwise velocity near the edge of the propeller jet causes the inboard vortices to be swept downstream past their original partner to interact with the second vortex encountered. Images of reduced contrast at  $J=0.3$  suggest that the vortices are swept to the third outboard partner downstream before interacting to swing out of the jet stream. Turbulent diffusion of the dye under these conditions, however, reduces the detectability of organized vorticity in the high velocity fluid.

It should be noted here that this strong wake instability should be greatly reduced in future experiments with constant propeller rotation. Despite the elimination of the shaft velocity perturbation, future experiments are expected to show strong dependence of the propeller wake evolution on  $J$ . This dependence stems from the inherent instability of the helix to perturbations (Widnall 1972), and the decrease in vortex spacing as  $J$  is decreased.

In particular, it will be interesting to note the variation in free surface influence on the breakdown of the helical form of the propeller wake as  $J$  is modified.

#### PROPELLER DEPTH VARIATION

Variation in the submerged depth of the propeller gave rise to two mutually interacting effects in the wake of the propeller. First, variations in wake vortical structure downstream are influenced by the presence of the free surface boundary condition. In addition, the free surface elevation is modified by surface piercing model support struts and local flow fluctuations. These local flow fluctuations are caused by proximity of either the propeller blades or their tip vortex wakes. The two depth variation influences will be treated separately in the sections to follow.

##### Propeller Wake Influence

The influence of the free surface on the vortical structures in the propeller wake appeared in this experiment in two forms. Variations in both the vortex trajectory and the size/brightness of the vortex spots were noted between the top and bottom illuminations of the wake. These variations were amplified as  $J$  or the non-dimensional submergence depth ( $z_{sub}/R$ ) were decreased.

A study of Fig. 12, showing a time sequence separated by 0.1 seconds at  $J=0.5$  and  $z_{sub}/R=1.25$  indicates the variation in vortex trajectory caused by proximity to the free surface. In this sequence the vortex labeled "1" moves much faster over the top of its partner labeled "2" than the corresponding vortex 3 moves below vortex 4. This difference could be a result of :

1. stronger vorticity in vortex 1 or 2 than in vortex 3 or 4  
(possibly due to reduced dissipation)

2. Stronger shear layer on top with respect to bottom (possible slight reverse flow on top due to zero friction boundary condition at surface)

Note that the movement of vortices "2" and "4" is relatively small.

Also notable in Fig. 12 is a distinct difference in both the shape and brightness of the dye spots marking the tip vortices. As mentioned earlier in the PROPELLER LOADING VARIATION section, the support struts show no influence on the dye visualization. The authors speculate, therefore, that the difference in dye diffusion between the top and bottom vortices is indicative of an influence of the free surface on the turbulent transition of the vortices. This is suggested by the stronger diffusion of dye near the edges of the vortices while the center spot stays bright longer. Velocity measurements in future experiments will shed light on this process.

#### Free Surface Influence

As mentioned earlier, the free surface elevation can be modified by the presence of several types of disturbances.

The model support struts piercing the free surface leave waves similar to those left by ships. These waves are dependent on the Froude number based on the speed of the carriage and chord length of the strut. Observations of the wave patterns behind the struts were made at a series of speeds between 1 and 4 ft/sec (0.305 and 1.22 m/sec) at the shallow submergence depth of  $z_{sub}/R=1.25$ . During these observations the  $J$  was set to 1.045 corresponding to the zero thrust condition for the purpose of minimizing propeller blade and wake effects on the free surface. These effects were examined separately as described in the next paragraph. The waves generated by the struts and pod are characterized in Table 1 below. The short wavelength transverse waves generated at 1

ft/sec (0.305 m/sec) decreased to an undetectable amplitude upstream of the propeller plane. In addition to increased dye visibility at this speed, the low strut influence was also a factor in conducting most of the observations at this speed.

The free surface effects due to propeller blade and wake vortex proximity were amplified expectedly as either the propeller submergence was decreased or the blade loading was increased. At  $z_{hub}/R=1.25$  surface depressions caused by blade passage became deep enough (for  $J<0.4$ ) to draw air from the surface and send it bubbling through the wake. It should be noted that this ventilation process was clearly distinguishable from a cavitation phenomenon which was not observed.

Surface seeding proved to be a limitation in examining the deflections at the air/water interface caused by wake vorticity. Dust particles proved to be very helpful in surface visualization. Strong currents created near the surface by the submerged vorticity, however, quickly cleared most of the particles deposited there. Remaining particles did indicate correlated free surface deflections with the dye marked vorticity below. The dynamic nature of the video image is necessary however to fully appreciate this correlation. Variations in the laser light intensity, caused by refraction angle changes at the free surface deflections, were also sensitive measurements of the influence of submerged vorticity on the free surface profile. When viewing the videotape, varying intensity bands in the laser light sheet can be traced to surface deflections. The small amplitude of these surface deflections under the conditions of this experiment are usually very difficult to see individually without the aid of these light rays.

## WAKE PERSISTENCE

An important motivation for this experiment was the examination of the persistence of the propeller wake a long time after the propeller had passed. Because only flow visualization measurements were being made, and the luminescence of the dye decreased below the video camera threshold after approximately 40 seconds at low  $J$  and 60 seconds at high  $J$ , no long term wake data could be recorded. To the eye; however, the fine dye gradients could be observed for over 4 minutes. Comments made here, will therefore be based on visual observations of the wake made by the authors during the actual testing. Two characteristic features were observed in the far wake of the propeller and they are described below.

The first feature noticed was the slow migration of the propeller wake jet towards the free surface. Once wake contact was made with the free surface, higher momentum fluid quickly moved upward forming strong axial surface currents. These currents were visible in movement of both the dye-diluted fluid near the surface and dust particles on the air/water interface. The downstream length for surface contact of the propeller wake with the surface ( $l_1$ ) is dependant on  $J$  and  $z_{hub}$ . The advance ratio essentially determines the wake spreading angle  $\beta$ , while  $z_{hub}/R$  defines an initial depth of the wake. The accurate measurement of  $l_1$  requires a precise and sensitive criterion for evaluating the wake/free surface interaction point. The velocity field due to a vortex, however prevents the definition of some range, beyond which no interaction exists. In future velocity measurement experiments, a threshold value for vortex wake induced velocities at the free surface will therefore be defined to signal an end point for  $l_1$ . Measurement of  $\beta$  was hampered in this experiment by the spacial variation in the wake edge caused by the

vortex twisting. A more analytic evaluation of the interdependence of these variables will therefore require additional measurements planned in the future.

Another feature noticed in the far wake was the intermittent occurrence of large turbulent structures long after the propeller had passed and most of the turbulent motion had diffused to low intensity. In several cases these structures were noticed up to 40 propeller diameters downstream. Velocity measurements may show additional intermittent turbulent structures of low intensity much farther downstream. It is not known what effect the improvement in propeller drive smoothness will have on the existence or strength of these persistent turbulent structures.

#### DISCUSSION AND RECOMMENDATIONS

The experiment described here included video recording of a range of propeller loadings and carriage speeds. In addition, limited video coverage of the 3-dimensional form of the helix was also obtained. The 3-dimensional form of the helix (Fig. 6) shows qualitatively the form of the instability present in the data reported in this paper.

Great care was taken to align the universal joints in setting up the experiment. No visual sign of the variation could be seen in the propeller even with a strobe light. Detailed measurements described in the HELIX INSTABILITY section showed however a 2.5 degree amplitude sinusoidal variation in the propeller shaft position causing blade loading and wake helix geometry variations of significant magnitude. An upgrade in the propeller drive design utilizes miter gears which will give constant velocity at the propeller shaft. A retesting of the propeller with the new drive gears will be carried out.

The authors suspect that once the shaft velocity variation is eliminated, a weaker instability will still be present in the wake helix due to either the free surface effects or

vortex breakdown. These influences should be more prominent in future experiments. Comparison of images from this experiment with those of round jet shear flows suggest that helical vortex geometry in the presence of its own strong shear layer may be unstable.

The implications of wake helix instability could have a significant effect on numerical wake analysis codes. The generation of more representative input mean and rms velocity files may be augmented by information on the spatial vorticity distribution. The presence of large scale vortical structures seen far downstream in the wake could play a significant role in energy storage and transfer to the free surface. The intermittent nature of these structures, however, may prevent accurate wake modeling by mean and rms quantities currently being used. The simultaneous use of flow visualization and Laser Doppler Velocimetry in future experiments will permit cost effective evaluation of the importance of these structures and their interactive nature with the free surface.

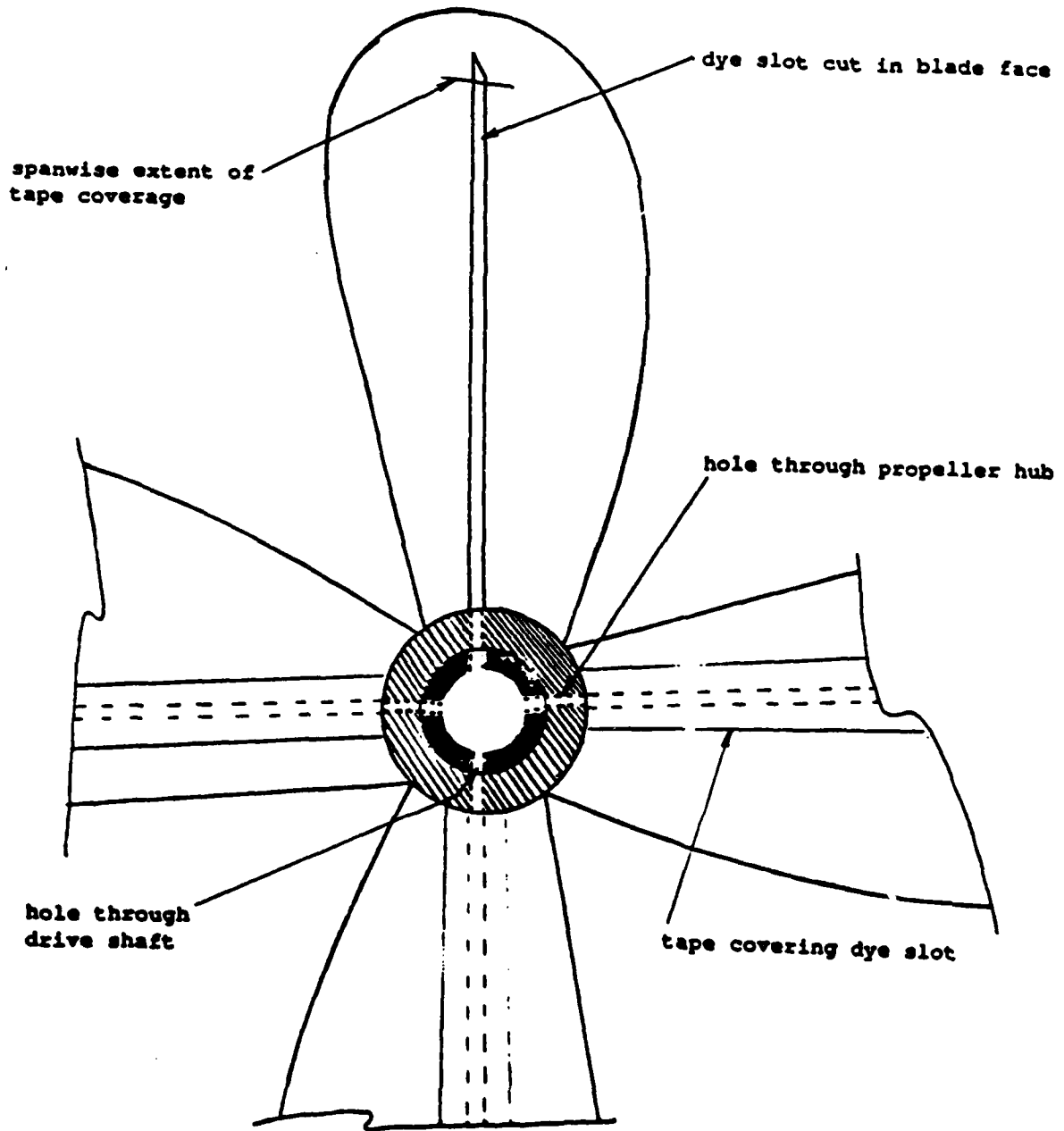


Fig 1. Four bladed propeller with hollow hub and dye slotted blades

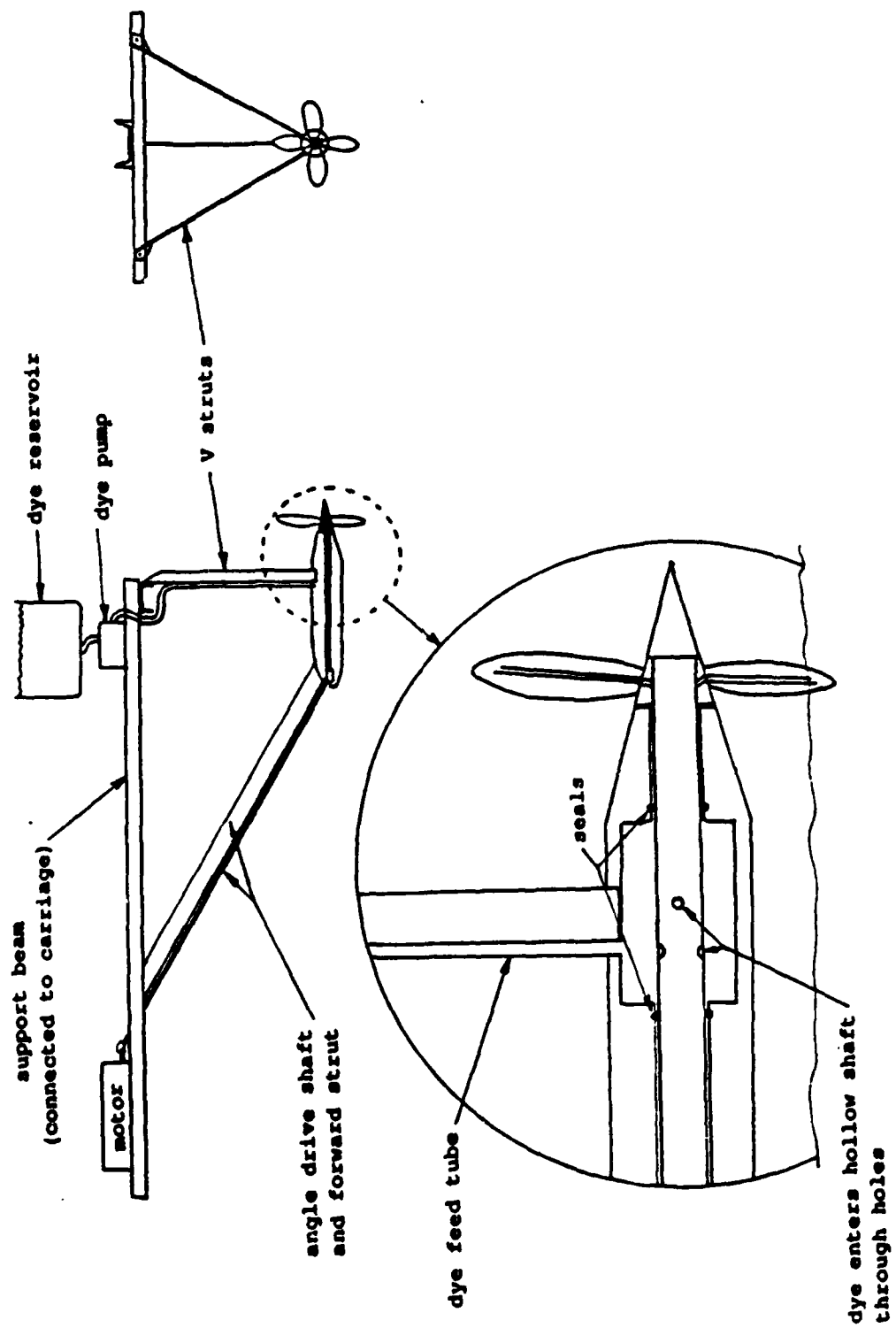


Fig 2. Experimental configuration

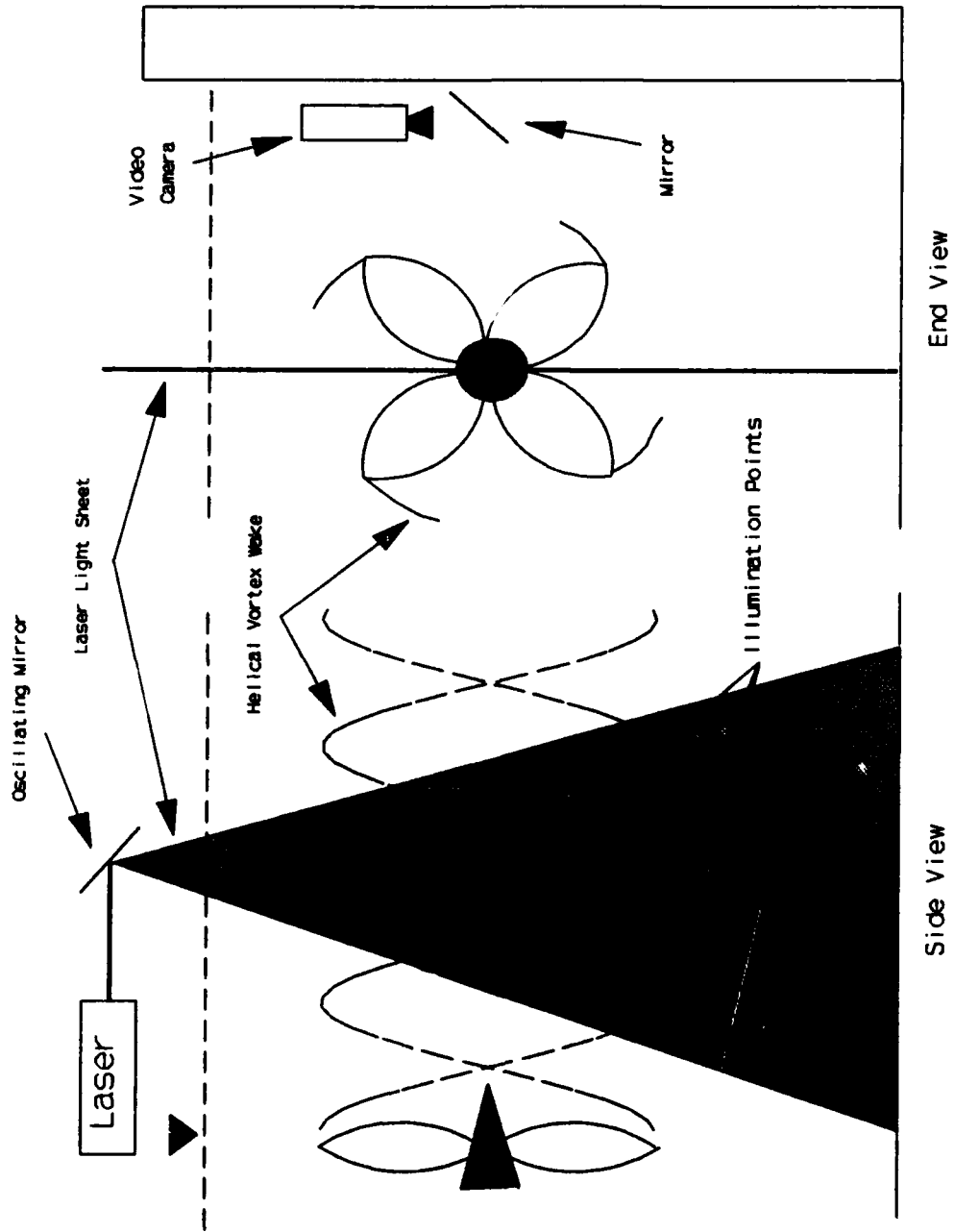


Fig. 3. Laser light sheet and video camera configuration

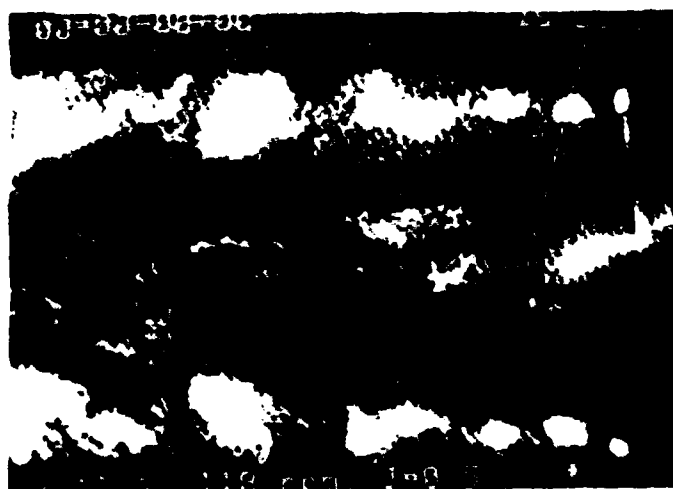
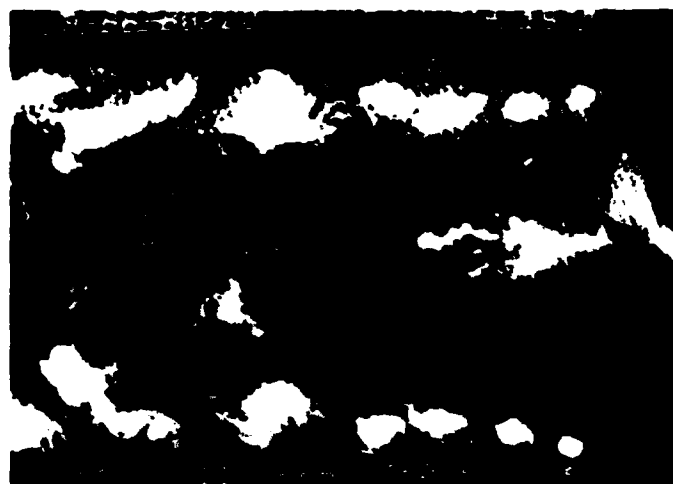
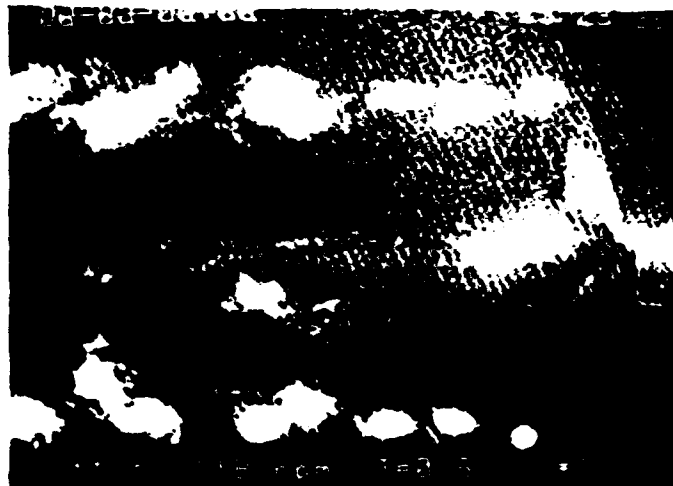


Fig. 4 - Video frames of vortex twisting,  $J=0.5$ , 0.1 second increments

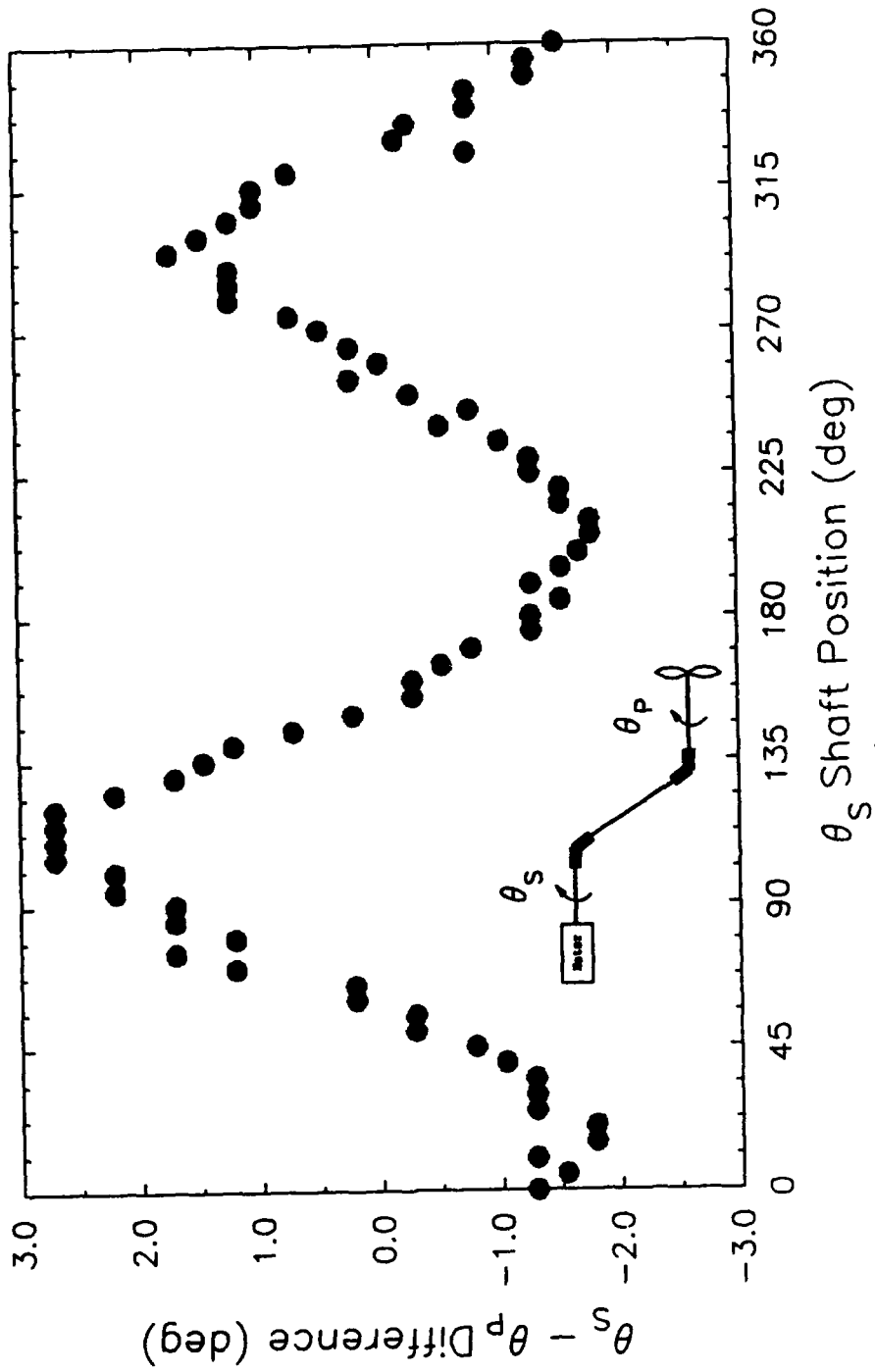
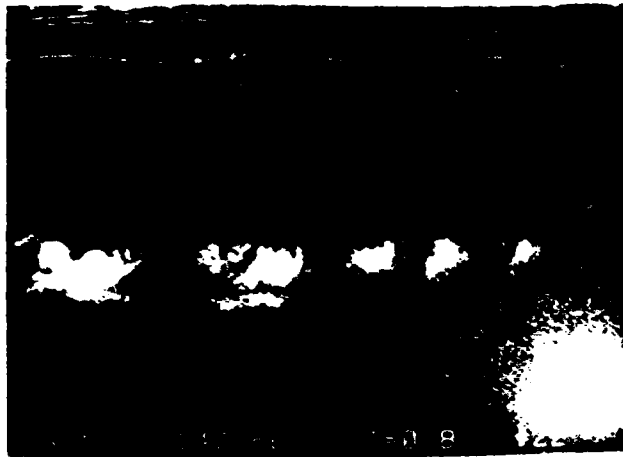


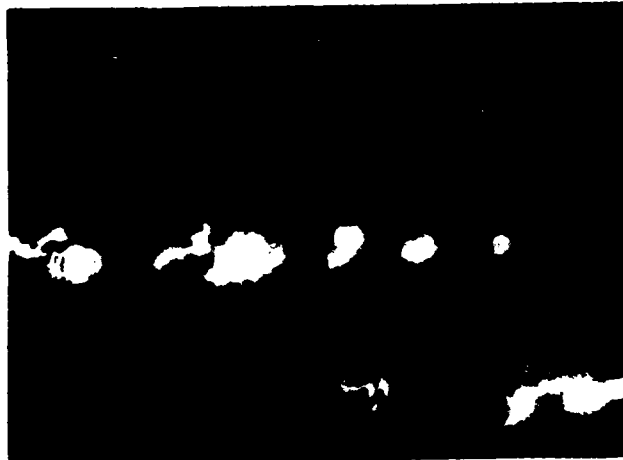
Fig. 5. Angular position of motor drive shaft and propeller



Fig. 6 - Three-dimensional view of tip vortex helix



$Re_{\alpha,7} = 1.3 \times 10^5$



$Re_{\alpha,7} = 1.95 \times 10^5$



$Re_{\alpha,7} = 2.6 \times 10^5$

Fig. 7 - Wake video frames for different  $Re_{\alpha,7}$

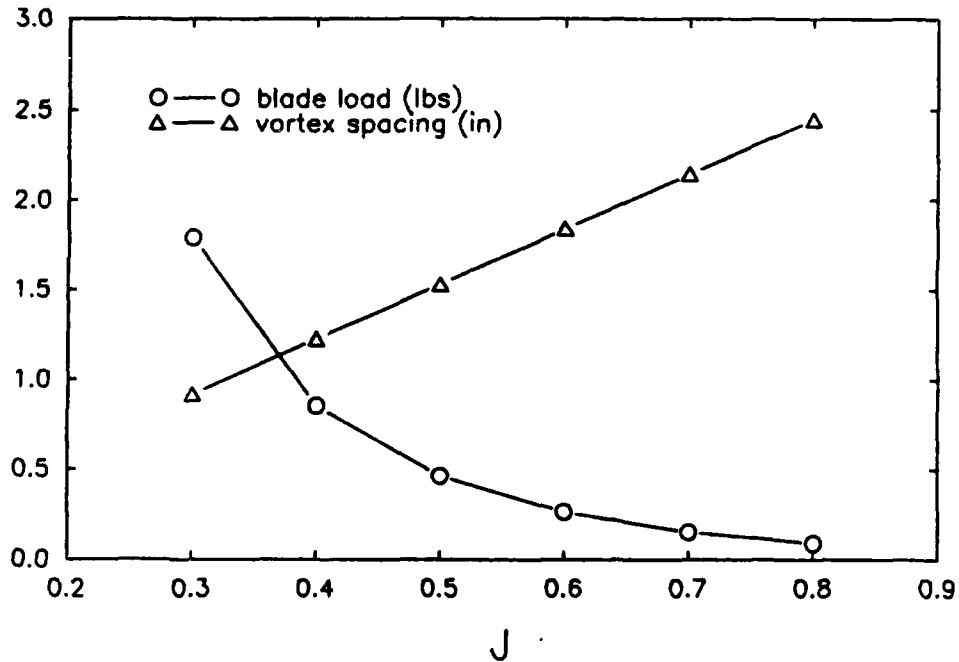


Fig. 9. Calculated blade loading and vortex spacing versus J

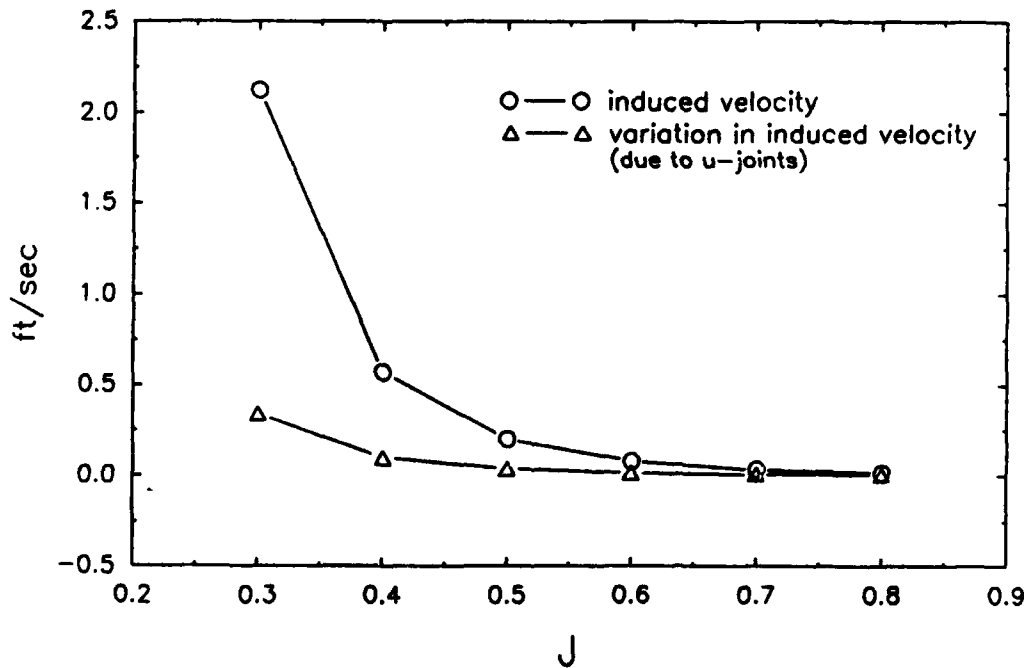
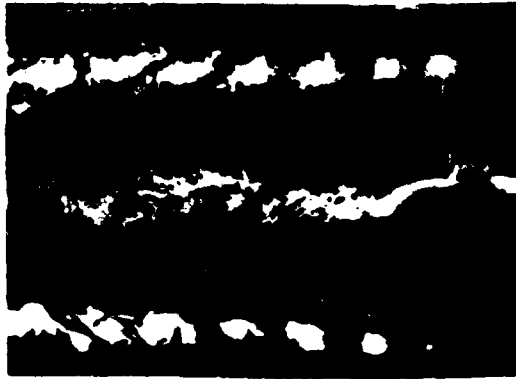
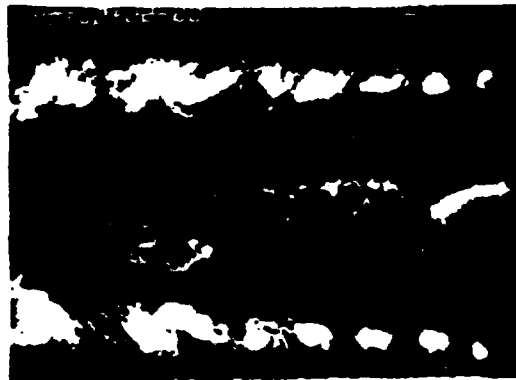


Fig. 10. Induced velocity variation



$J = 0.8$



$J = 0.6$



$J = 0.5$



$J = 0.4$

Fig. 8 - Wake video frames:  $J$  variation,  $z_{max}/R=2.0$

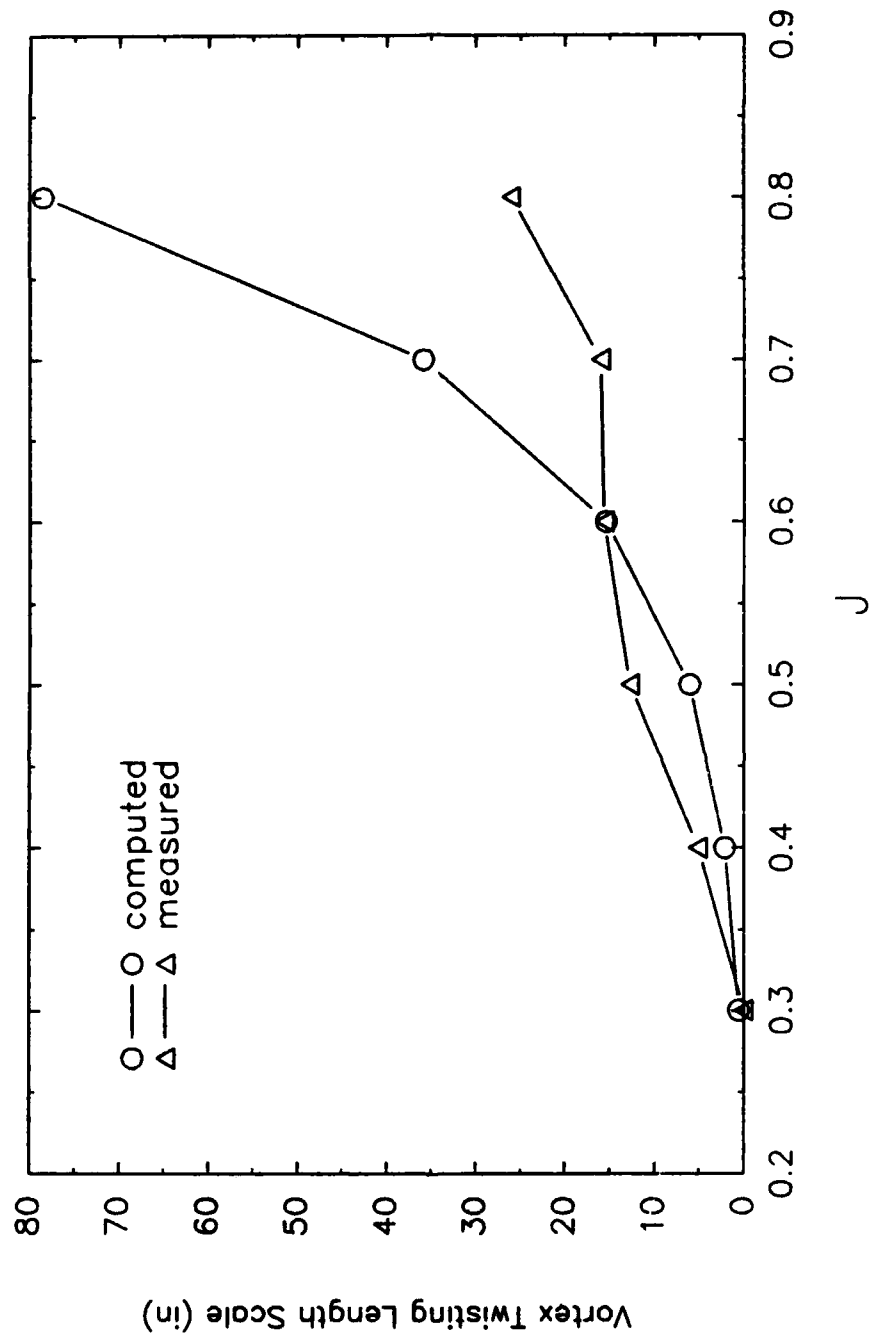


Fig. 11. Comparison of calculated and measured streamwise wake length scale

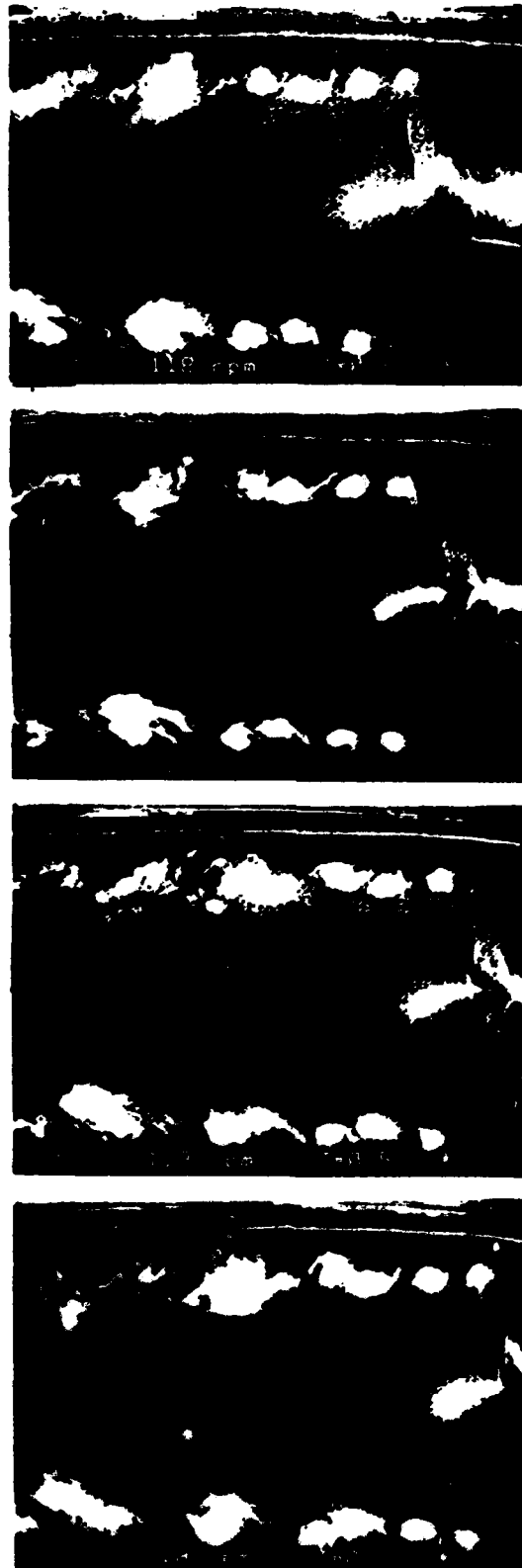


Fig. 12. Wake video frames: shallow submergence,  $z_{sub}/R=1.25$ ,  $J=0.5$

Table 1. Free surface effects due to struts and pod:  $z_{pod}/R=1.25$

---

Carriage Speed (ft/sec)	Wave Pattern
1	Short 1.5 in. (4 cm) wavelength divergent waves due to the struts: amplitude < 0.5 in. (1 cm).
2	Diverging and transverse waves of approximately 8 in. (20 cm) wavelength $\approx$ 0.75 in. (2 cm) amplitude.
3	Dominant transverse wave system due to pod: wavelength $\approx$ 2 ft (0.6 m) and amplitude $\approx$ 0.8 in. (2 cm) due to pod.
4	Dominant transverse wave system: wavelength $\approx$ 3.5 ft (1.1 m) and amplitude $\approx$ 1 in. (2.5 cm) due to pod.

---

## REFERENCES

- Blanton, J.N., and S. Fish (1988), "Near and Far Field Propeller Wake Study Using Laser Doppler Velocimetry", DTRC/SHP-1268-01.
- Cimbala, J.M., H.M. Nagib, and A. Roshko (1988), "Large structure in the Far Wakes of Two-dimensional Bluff Bodies", *J. Fluid Mech.*, vol. 190, pp. 265-298.
- Cook, C.V. (1972), "The Structure of the Rotor Blade Tip Vortex", AGARD Proceedings on Aerodynamics of Rotary Wings.
- Fish, S. and J.N. Blanton (1988) "Propeller Wake Flow Visualization Near a Free Surface", DTRC/SHP-1268-02.
- Greeley, D.S., and J.E. Kerwin (1982), "Numerical Methods for Propeller Design and Analysis in Steady Flow", *SNAME Transactions*, vol. 90, pp 415-453.
- Hama, F.R. (1962), "Streaklines in a Perturbed Shear Flow", *Physics of Fluids*, vol. 5, number 6.
- Ho, C.M., and P. Huerre (1984), "Perturbed Free Shear Layers", *Ann. Rev. Fluid Mech.*, vol. 16, pp. 365-424.
- Kuiper, G. (1979), "Modeling of Tip Vortex Cavitation on Ship Propellers", 4<sup>th</sup> Lips Propeller Symposium, Drunen-The Netherlands.
- Lugt, H.J. (1959), "Einfluss der Drallströmung auf die Durchflusszahlen genormter Drosselmessgeräte", PhD Thesis, Stuttgart, Partially translated by the British Hydromechanics Research Association, Rep. T 716 (February 1962).
- Lyden, J.D., D.R. Lyzenga, R.A. Shuchman, and E.S. Kasischke (1985), "Analysis of Narrow Ship Wakes in Georgia Strait SAR Data", E.R.I.M. report # 155900-20-T, Ann Arbor, MI.
- Moore, D.W. (1971), "The Discrete Vortex Approximation of a Finite Vortex Sheet", Calif. Inst. Tech. Rep. AFOSR-1804-69.
- Meyne, K. (1972), "Investigation of Propeller boundary-layer flow and Friction Effect on Propeller Characteristics", DTNSRDC Trans-352.
- Widnall, S. E. (1972), "The Stability of a Helical Vortex Filament", *J. Fluid Mech.*, Vol. 54, Part 4.